Non-invasive delivery of biological macromolecular drugs into the skin by iontophoresis and its application to psoriasis treatment

Tatsuya Fukuta,[1,#] Yasufumi Oshima,[1,#] Kohki Michiue, Daichi Tanaka, Kentaro Kogure[1,*]

[1]*Department of Pharmaceutical Health Chemistry, Graduate School of Biomedical Sciences, Tokushima University, Shomachi 1, Tokushima 770-8505, Japan*

[*]Correspondence author: Kentaro Kogure

TEL: +81-88-633-7248

FAX: +81-88-633-9572

Email: kogure@tokushima-u.ac.jp

Department of Pharmaceutical Health Chemistry, Graduate School of Biomedical Sciences, Tokushima University, Shomachi 1, Tokushima 770-8505, Japan

[#]These authors contributed equally to this work

Abstract

Biological macromolecular drugs, such as antibodies and fusion protein drugs, have been widely employed for the treatment of various diseases. Administration routes are typically via invasive intravenous or subcutaneous injection with needles; the latter is challenging for applications involving inflamed skin (e.g., psoriasis) due to concerns of expansion of inflammation. As a method of non-invasive transdermal drug delivery, we previously demonstrated that iontophoresis (IP) using weak electric current (0.3-0.5 mA/cm^2) enables transdermal permeation of hydrophilic macromolecules, such as small interfering RNA and nanoparticles into the skin, and subsequent exertion of their functions. The underlying mechanism was revealed to be via intercellular junction cleavage by cellular signaling activation initiated by Ca^{2+} influx. Based on these findings, in the present study, we hypothesized that non-invasive intradermal delivery of biological macromolecular drugs could be efficiently achieved via IP. Fluorescence of FITC-labeled IgG antibody was broadly observed in the skin after IP administration (0.4 mA/cm^2 for 1 h) and extended from the epidermis to the dermis layer of hairless rats; passive antibody diffusion was not observed. In imiquimod-induced psoriasis model rats, antibodies were also delivered via IP into inflamed skin tissue. Additionally, upregulation of interleukin-6 mRNA levels, which is related to pathological progression of psoriasis, was significantly inhibited by IP of the anti-tumor necrosis factor-α drug etanercept, but not by its subcutaneous injection. Importantly, IP administration of etanercept significantly ameliorated epidermis hyperplasia, a symptom of psoriasis. Taken together, the present study is the first to demonstrate that IP can be applied as a non-invasive and efficient intradermal drug delivery technology for biological macromolecular drugs.

Keywords

Iontophoresis; Transdermal drug delivery; Biological macromolecular drugs; Antibody; Psoriasis; Inflammation

1. **Introduction**

In recent years, biological macromolecular drugs, such as antibodies and fusion protein drugs, have been developed and employed for the treatment of various diseases, including cancer and inflammatory diseases [1-3]. A therapeutic advantage of biological macromolecular drugs in comparison to conventional low molecular weight drugs is that the former can exert high therapeutic benefit with fewer side effects by selectively binding to or capturing their target molecules. Most administration routes for biological macromolecular drugs have been via systemic delivery by intravenous or subcutaneous injection with needles. While injection is generally recognized as an instantaneous and effective administration method, there are several problems with injection methods, such as invasiveness, pain, and risk of infection due to repeated use of a needle, which leads to concerns of decreased patient compliance [4-6]. Also, skilled techniques are often required for secure injection.

Psoriasis is an autoimmune disease that follows chronic courses with inflammatory symptoms of the skin, and is typically treated using biological macromolecular drugs [7, 8]. Although the specific causes of the disease have not yet been elucidated, it has been reported that excess production of inflammatory cytokines, such as interleukin (IL)-1, IL-6, IL-8, tumor necrosis factor (TNF)-α, and interferon-γ, around the diseased site is involved in pathological progression of psoriasis [8]. Among these inflammatory cytokines, TNF-α has been demonstrated to be an important therapeutic target in psoriasis, and various biological macromolecular drugs, including antibody agents such as infliximab, adalimumab, and the anti-TNF-α drug etanercept, represent effective therapeutic agents for psoriasis [9, 10]. Most of these agents are administered by injection, specifically subcutaneous (*s.c.*) injection. However, administration of these agents to abnormal skin, including psoriatic eruption, is often avoided due to the risk of inflammatory expansion, thus limiting the site where *s.c.* injection can be performed. In addition, the administration site must be changed for each subsequent injection. Moreover, needle insertion for *s.c.* injection often results in vascular inflammation, and is associated with a risk of adverse skin effects (e.g., redness and rash) at the injection site [11]. Hence, development of a new method capable of non-invasive and efficient delivery of biological macromolecular drugs into psoriatic inflamed skin is needed to mitigate the above-mentioned problems.

To increase transdermal drug delivery efficiency, several physical technologies including iontophoresis (IP) [12, 13], electroporation [14], sonophoresis [15], and microneedles [16], have been reported. Among these technologies, we have focused on IP using weak electric current (0.3-0.5 mA/cm^2), which offers a simple and non-invasive method compared with other methods, as needles and other complicated devices are not required. IP can be used to promote transdermal permeation of charged molecules into skin tissue. However, IP has typically been considered to be applicable only for charged low molecular weight compounds with relatively high hydrophobicity via electrorepulsion and electroosmosis [17]. We recently succeeded in the intradermal delivery of hydrophilic macromolecular drugs, including small interfering RNA (siRNA; M.W. ca. 12,000) and CpG oligo DNA (M.W. ca. 6,600) via IP, and demonstrated successful exertion of their functions *in vivo* (i.e., RNA interference and immune-activation, respectively) [18, 19]. In our previous studies, we also reported that nanoparticles, such as insulin-encapsulating liposomes and antigen peptide-loaded nanogels, can also be intradermally delivered via IP [20, 21]. The mechanism of IP-mediated permeation of hydrophilic macromolecules and nanoparticles into skin tissues was previously revealed to involve Ca^{2+}-mediated intracellular signal activation induced in skin cells by IP, followed by decreased expression of gap-junction protein Cx43 and depolymerization of polymerized actin, a tight junction associated protein, resulting in intercellular junction cleavage [22]. An advantage of IP-mediated drug delivery is that intradermally delivered drugs via IP are gradually released into the systemic circulation while maintaining a certain concentration in the blood upon sustained movement from the skin tissue to the circulation, by the skin acting as a reservoir [12]. Based on these findings, we hypothesized that IP could offer a non-invasive, safe, and efficient transdermal technology for delivery of biological macromolecular drugs, such as antibodies and fusion protein drugs, which typically exhibit very high molecular weights (ca. ≥150,000). Moreover, IP may be able to be applied for the treatment of psoriasis as an alternative to invasive *s.c.* injection.

In the present study, we examined the transdermal delivery into skin tissue via IP of an antibody as a representative biological macromolecular drug. We employed a previously reported psoriasis rat model [23, 24] to investigate whether the antibody can also be delivered into the psoriatic inflamed skin tissue by IP. Finally, we evaluated the functionality of the anti-TNF-α drug etanercept (recombinant human TNF-α receptor: Fc fusion protein), delivered via IP into the skin of the psoriasis model rats. We compared the effectiveness of IP-mediated etanercept administration with that of *s.c.* injection, which is the conventional administration route for psoriasis treatment.

2. Methods

2.1. Animals

Male HWY hairless rats (190-210 g) were purchased from Japan SLC, Inc. (Shizuoka, Japan) and were 7 weeks old at the beginning of each experiment. All animal experiments were evaluated and approved by the Animal and Ethics Review Committee of Tokushima University.

2.2. Iontophoresis (IP) of fluorescent-labeled antibody

IP of antibodies was performed in accordance with our previous reports [22]. Briefly, normal HWY hairless rats were anesthetized by intraperitoneal injection of chloral hydrate (400 mg/kg rat) dissolved in phosphate-buffered saline (PBS). To administer fluorescein isothiocyanate (FITC)-labeled IgG antibody (Sigma-Aldrich, Tokyo, Japan), nonwoven fabric (2.25 cm^2) containing 1 mg (200 µL) of FITC-labeled IgG solution (5 mg/mL) was placed on the dorsal skin, and a nonwoven fabric moistened with 200 µL of PBS was also placed 1 cm away. Each piece of nonwoven fabric containing IgG and PBS was attached to Ag-AgCl electrodes (3M Health Care, Minneapolis, MN, USA) with surface areas of 2.25 cm^2. The Ag-AgCl electrodes with nonwoven fabric containing FITC-labeled IgG or PBS were connected to the cathode and anode, respectively, of a power supply (TTI ellebeau, Inc., model TCCR-3005, Tokyo, Japan). After covering the connections with tape, IP was performed with a constant current of 0.4 mA/cm^2 (0.9 mA) for 1 h.

2.3. Intradermal distribution of fluorescent-labeled antibody after IP

At 0 or 3 h after 1-h IP of FITC-labeled IgG as described above, the skin of the rats was removed, embedded in optimal cutting temperature (OCT) compound (Sakura Finetek, Tokyo, Japan), and then frozen with dry ice/ethanol. The frozen skin sections were cut into 10-µm thick sections using a cryostat (CM3050S; Leica Biosystems, Tokyo, Japan). The 10-µm thick frozen sections were mounted onto MAS-coated slide glasses with Perma Fluor Aqueous Mounting Medium (Thermo

Fisher Scientific, Waltham, MA, USA). FITC fluorescence of the skin sections was observed with a confocal laser scanning microscope (LSM700, Carl Zeiss, Jena, Germany).

2.4. Immunostaining of intercellular junction proteins

The 10-μm thick frozen skin sections were immunostained for a gap junction protein connexin 43 (Cx43), an intercellular junction protein. Briefly, the sections were fixed with 4% paraformaldehyde (PFA) for 15 min at room temperature, and incubated with 1% bovine serum albumin (BSA) in PBS for 20 min at room temperature. Then, the sections were incubated with rabbit anti-Cx43 antibody (ab11370, Abcam, Cambridge, UK) at a dilution of 1:100 at 4ºC overnight. Next, the sections were incubated with Alexa 647-conjugated goat anti-rabbit IgG antibody (ab150079; Abcam) at a dilution of 1:200 for 60 min at 37ºC. After mounting with Perma Fluor Aqueous Mounting Medium, the fluorescence in the sections was observed by confocal laser scanning microscopy.

2.5. Preparation of psoriasis model rats

Psoriasis model rats were prepared as previously reported [23]. Briefly, 7-week-old hairless rats were anesthetized with 3% isoflurane (Escain®, Pfizer, NY, USA) and maintained with 1.5% isoflurane. Under isoflurane anesthesia, 60 mg of imiquimod (IMQ) cream (5%; Beselna cream; Mochida Pharmaceuticals, Tokyo, Japan) was topically applied onto the dorsal skin of rats, after which the rats were allowed to recover from anesthesia. IMQ treatment was performed 4 times per 24 h to induce psoriasis, and the resultant rats were used in the following experiments.

2.6. Hematoxylin-eosin (HE) staining of inflamed skin of the psoriasis model

To confirm induction of psoriasis, the skin of the rats treated with IMQ cream for 4 days was removed at day 8 after the start of IMQ treatment (day 1), and the frozen skin sections (10 μm) were prepared as described above. The sections were then fixed with 4% PFA for 10 min. After washing with PBS, the sections were stained with Mayer's hematoxylin solution (Fuji Film Wako Pure Chemical, Osaka, Japan) for 10 min at room temperature, and subsequently with 1% eosin (Fuji Film Wako Pure Chemical) for 1 min at room temperature. The samples were then dehydrated with 80-100% ethanol, cleared with xylene, and mounted with hydrophobic mounting medium (Entellan®New, Merck Millipore, Burlington, MA, USA). Finally, the sections were observed using a fluorescence phase contrast microscope (BZ-9000, Keyence, Osaka, Japan).

2.7. Intradermal distribution of IP-delivered FITC-labeled antibody in psoriatic skin

At 24 or 72 h after the 4th IMQ treatment on the dorsal skin of hairless rats, IP administration of FITC-labeled IgG was carried out as described above (2.2. Iontophoresis (IP) of fluorescent-labeled antibody). Three hours after each treatment with FITC-labeled IgG, 10-μm frozen sections of the psoriatic inflamed skin were prepared. Following the addition of 4',6-diamidino-2-phenylindole (DAPI) solution (1.0 μg/mL, Thermo Fisher Scientific) onto the sections, the sections were then mounted with Perma Fluor Aqueous Mounting Medium. The fluorescence of FITC and DAPI in the skin sections was observed by confocal laser scanning microscopy.

2.8. IP of biological macromolecular drugs onto the psoriasis model

IMQ cream-induced psoriasis model rats were anesthetized with chloral hydrate (400 mg/kg rat). Nonwoven fabric (2.25 cm^2) containing 1 mg (200 μL) of a solution of the anti-TNF-α drug etanercept (recombinant human soluble TNF-α receptor: Fc fusion protein) was attached to Ag-AgCl electrodes with surface area of 2.25 cm^2, and applied onto the skin to induce psoriatic inflammation. The Ag-AgCl electrodes with nonwoven fabric containing etanercept or PBS were connected to the cathode and anode of a power supply, respectively. After covering the connections with tape, IP was performed with a constant current of 0.4 mA/cm^2 (0.9 mA) for 1 h. The iontophoretic administration of etanercept was performed 24 and 72 h after the 4th IMQ treatment on the dorsal skin of hairless rats. Twenty-four hours after the 2nd IP treatment, the skin under the cathode was removed and total RNA was isolated as described in the following section to evaluate the function of IP-delivered etanercept.

2.9. RNA extraction

The skin of each IMQ-induced psoriasis model rat in each group was removed and immersed in Allprotect Tissue Reagent (QIAGEN, Hilden, Germany) to stabilize RNA before extraction. Next, 250 mg of the cut skin tissue was homogenized in 5 mL of QIAzol Lysis reagent (QIAGEN) using a TissueRuptor II (QIAGEN). After 5 min of incubation at room temperature, total RNA was purified and extracted with an RNeasy Plus Universal Midi kit (QIAGEN) according to the manufacturer’s instructions. The total RNA concentration was quantified using a Nanodrop 8000 (Thermo Fisher Scientific).

2.10. Quantitative analysis of mRNA expression of inflammatory cytokines by real-time reverse transcription polymerase chain reaction (RT-PCR)

cDNA was synthesized from 200 ng of total RNA with PrimeScript RT Master Mix (Perfect Real Time, Takara Bio, Otsu, Japan) and an MJ Mini Personal Thermal Cycler (Bio-Rad, Hercules, CA, USA). The conditions for the reverse transcription reaction were 37℃ for 15 min, whereas those for inactivation of reverse transcriptase were 85ºC for 5 sec. Real-time RT-PCR analysis was performed using TB Green™ Premix Ex Taq™ II (Tli RNaseH Plus, Takara Bio) and a Thermal Cycler Dice Real Time System III (Takara Bio). To analyze the mRNA expression levels of TNF-α, IL-6, and GAPDH, the cDNA was denaturated at 95ºC for 30 sec, followed by 40 cycles of 95ºC for 5 sec and 60ºC for 30 sec for amplification. The sequences of the primers used for the real-time RT-PCR are shown in Table 1. The mRNA levels of TNF-α and IL-6 were calculated using the $2^{-\Delta\Delta Ct}$ method by normalization relative to GAPDH mRNA. The relative transcript levels (TNF-α/GAPDH mRNA and IL-6/GAPDH mRNA) were calculated to compare differences between each group.

2.11. Evaluation of epidermis thickness

HE staining was performed for the 10-μm frozen skin tissues of psoriasis model rats in each treatment group, as described above (2.6. Hematoxylin-eosin (HE) staining of inflamed skin of the psoriasis model). Then, the sections were observed with a fluorescence phase contrast microscope (BZ-9000), and average epidermis thickness was calculated from over 20 images per rat by using an image analysis application of BZ-9000.

2.12. Statistical analysis

Statistical differences were evaluated by one-way analysis of variance with the Tukey *post-hoc* test. Comparison between two groups were determined using the Student's *t*-test. Data are presented as mean ± standard deviation (S.D.).

Table 1. Primer sequences for real-time RT-PCR.

Gene	Forward	Reverse
GAPDH	CCCCCAATGTATCCGTTGTG	TAGCCCAGGATGCCCTTTAGT
TNF-α	CGTAGCAAACCACCAAGCA	CGTAGCAAACCACCAAGCA
IL-6	TCCTACCCCAACTTCCAATGCTC	TTGGATGGTCTTGGTCCTTAGCC

3. Results

3.1. Intradermal distribution of FITC-labeled IgG delivered via iontophoresis

We performed transdermal delivery of FITC-labeled IgG (M.W. ca. 150,000) via IP on the dorsal skin of hairless rats. Fluorescence was hardly observed in the skin tissues at 3 h after treatment for both topical skin application of FITC-IgG alone onto the skin (i.e., passive diffusion) and iontophoretic treatment alone (Figs. 1A and B). On the other hand, when FITC-IgG solution was administered via IP, fluorescence was clearly observed around the epidermis immediately after 1-h IP (Fig. 1C), as judged from the image of the HE-stained skin in Fig. 1F. Surprisingly, broad fluorescence of the antibody was observed extending from the epidermis layer to the dermis layer at 3 h after IP-mediated delivery of the antibody (Figs. 1D and E). In addition, to quantify the amount of FITC-IgG administered via IP, we harvested the nonwoven fabric, in which FITC-IgG was impregnated, attached onto cathodal Ag-AgCl electrode immediately after 1-h IP, and immersed in 1 mL PBS to extract FITC-IgG retained in the nonwoven fabric. Then, the FITC fluorescence in extract was measured. The results showed that the retained FITC-IgG in nonwoven fabric after IP was 16.4 ± 1.1% (n=3) of applied FITC-IgG, suggesting that approximately 80% of the FITC-IgG could be administered by IP. These results suggest that antibodies, which are very large molecules with high hydrophilicity, can be successfully delivered into skin tissue by IP.

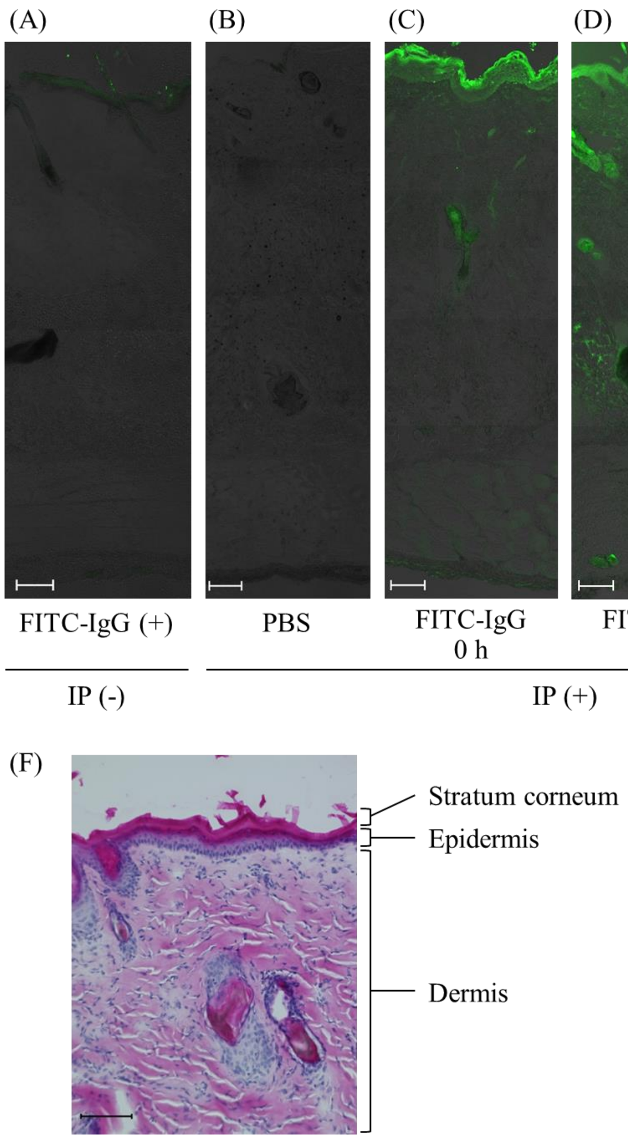

Fig. 1. Intradermal distribution of fluorescent-labeled antibody delivered by iontophoresis (IP).

Confocal images of 10-μm frozen skin sections of hairless rats applied with FITC-IgG without IP (0.4 mA/cm2) for 3 h (A; n=3) and 3 h after treatment by 1-h IP alone (B; n=3). The hairless rats were also transdermally administered FITC-IgG via 1-h IP. At 0 h (C; n=4) and 3 h (D and E; n=4) after 1-h IP, FITC fluorescence was observed by confocal microscopy. Scale bars = 100 μm. Image of dorsal skin tissue of hairless rats stained with HE (F). Stratum corneum, epidermis, and dermis. Scale bar = 100 μm.

We next performed immunostaining for an intercellular gap junction protein, connexin 43 (Cx43), to confirm the induction of intercellular junction cleavage via IP and to observe the relationship between intradermal distribution of FITC-IgG delivered by IP and Cx43 expression. The confocal images showed that the expression of Cx43 was widely observed in the skin tissue not treated by IP (Fig. 2A). IP treatment induced obvious reduction of Cx43 expression (Fig. 2B), similar to our previous report [22]. Importantly, the fluorescence of FITC-IgG was remarkably observed in the region where the Cx43 expression decreased around both the epidermis and dermis layers (Fig. 2C). These results suggest that FITC-IgG could be permeated into skin tissue by IP through the cellular gap derived from cleaved intercellular junction by IP treatment.

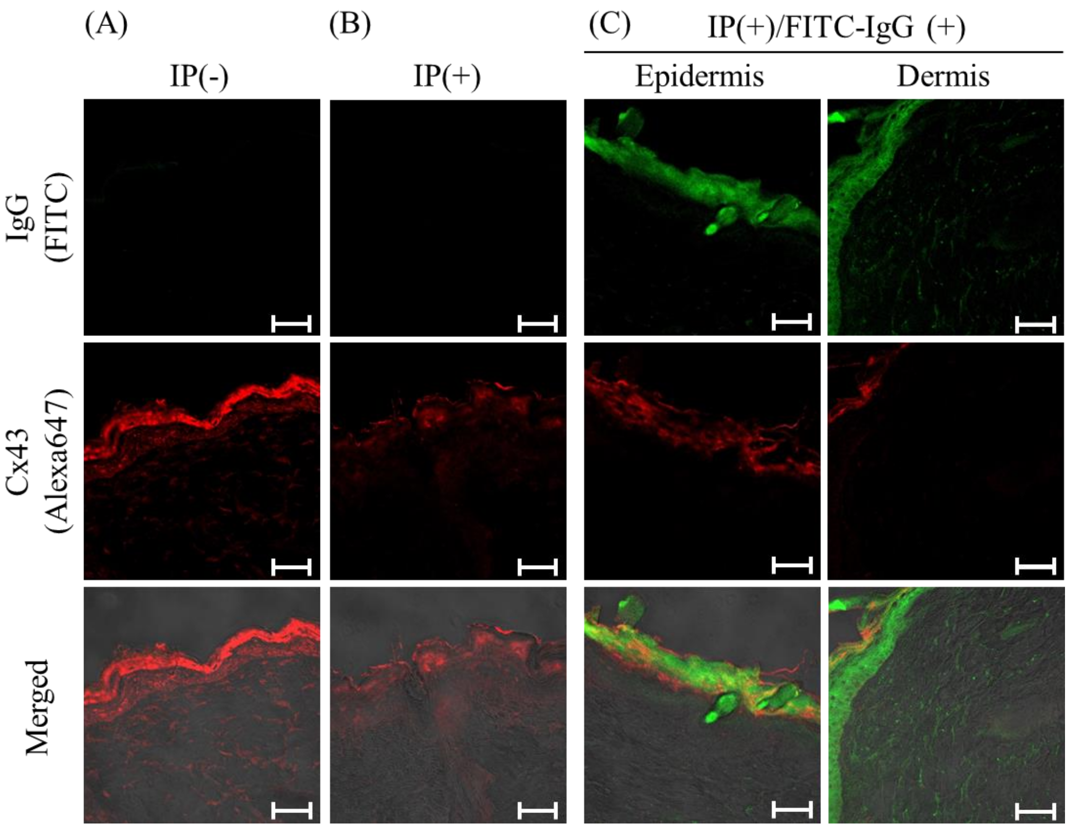

Fig. 2. Transdermal permeation of fluorescence-labeled antibody via the cleaved intercellular junctions induced by IP.

The rats were transdermally administered FITC-IgG via 1-h IP. Three hours after 1-h IP, the skins of the rats were dissected, and 10-μm frozen sections were prepared, followed by immunostaining for an intercellular gap junction protein Cx43. The fluorescence images of the skin were obtained by confocal laser scanning microscopy. The images of the skin sections (A; IP (-)), (B; IP (+)/FITC-IgG (-), (C) IP (+)/FITC-IgG (+)) are shown. (C) The images in left column indicate the images obtained around the epidermis and those in right column around the dermis. Green and red indicate FITC (IgG) and Alexa647 (Cx43), respectively. Merged images of FITC, Alexa647, and blight field are shown. Scale bars = 50 μm. The experiments were independently performed three times.

3.2. Preparation of IMQ-induced psoriasis model and IP-mediated delivery of antibodies into psoriatic skin

Following the successful transdermal delivery of biological macromolecular drugs by IP, we examined whether this macromolecular delivery technology can be employed for therapeutic application against an inflammatory disease, namely psoriasis, which is typically treated with biological macromolecular drugs. Following repeated treatment of the dorsal skin with IMQ for a total of 4 times, induction of psoriatic inflammation was histologically examined by HE staining. As shown in the images of HE-stained skin in Figs. 3A and B, hyperplasia of the epidermis was clearly observed for IMQ-induced psoriasis compared with non-treated normal rats, suggesting that the psoriasis model was successfully prepared in accordance with previous reports [23, 24].

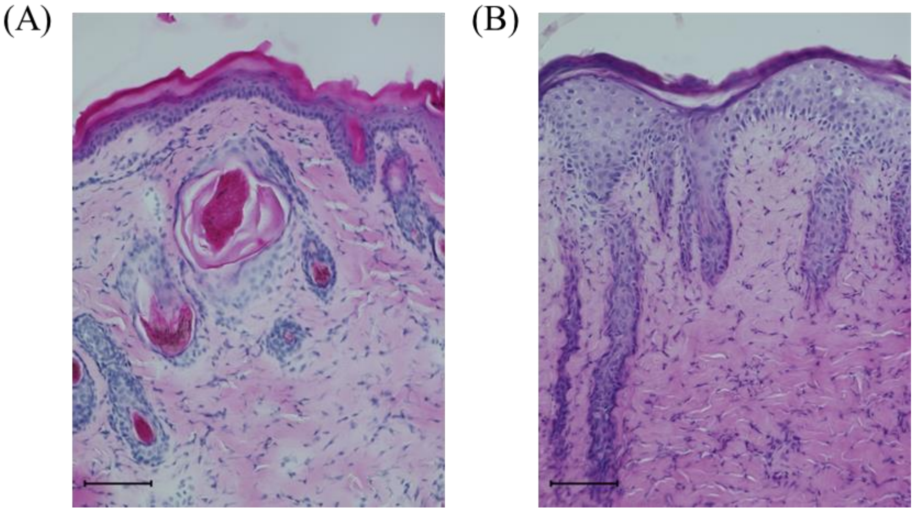

Fig. 3. Evaluation of psoriatic skin inflammation in IMQ-induced psoriasis model rats.

The psoriasis model rats were prepared by topical application of IMQ cream (60 mg/rat/treatment) a total of four times. Eight days after the 1st IMQ treatment (day 1), 10-µm frozen skin sections were prepared, and HE staining was performed. Microscopic images of skin sections from normal (A) and IMQ-treated psoriasis model rats (B). Scale bars = 100 µm.

Using this psoriasis model, we investigated the intradermal distribution of FITC-IgG administered by IP. As shown in Fig. 4A, topical skin application of FITC-IgG alone (passive diffusion), IP alone, and IP of FITC-IgG was performed 24 h after the 4^{th} IMQ treatment, whereas IP of FITC-IgG was conducted twice in the other group of rats at 24 and 72 h after the last IMQ treatment. Confocal images, which were obtained from skin sections prepared 3 h after each treatment, showed no FITC fluorescence in the groups with topical skin application of FITC-IgG or IP alone (Figs. 4B and C). Further, the fluorescence derived from FITC-IgG was prominently detected by IP-mediated administration of the antibody (Fig. 4D). In an effort to deliver the antibody more reliably, two doses of the antibody IP were carried out and the subsequent intradermal distribution was observed. Similar to the results obtained using the single dose, FITC fluorescence was strongly detected in the psoriatic skin (Fig. 4E). Taken together, these results suggest that IP can be applied for intradermal delivery of biological macromolecular drugs, such as antibodies, even in the setting of inflammatory skin.

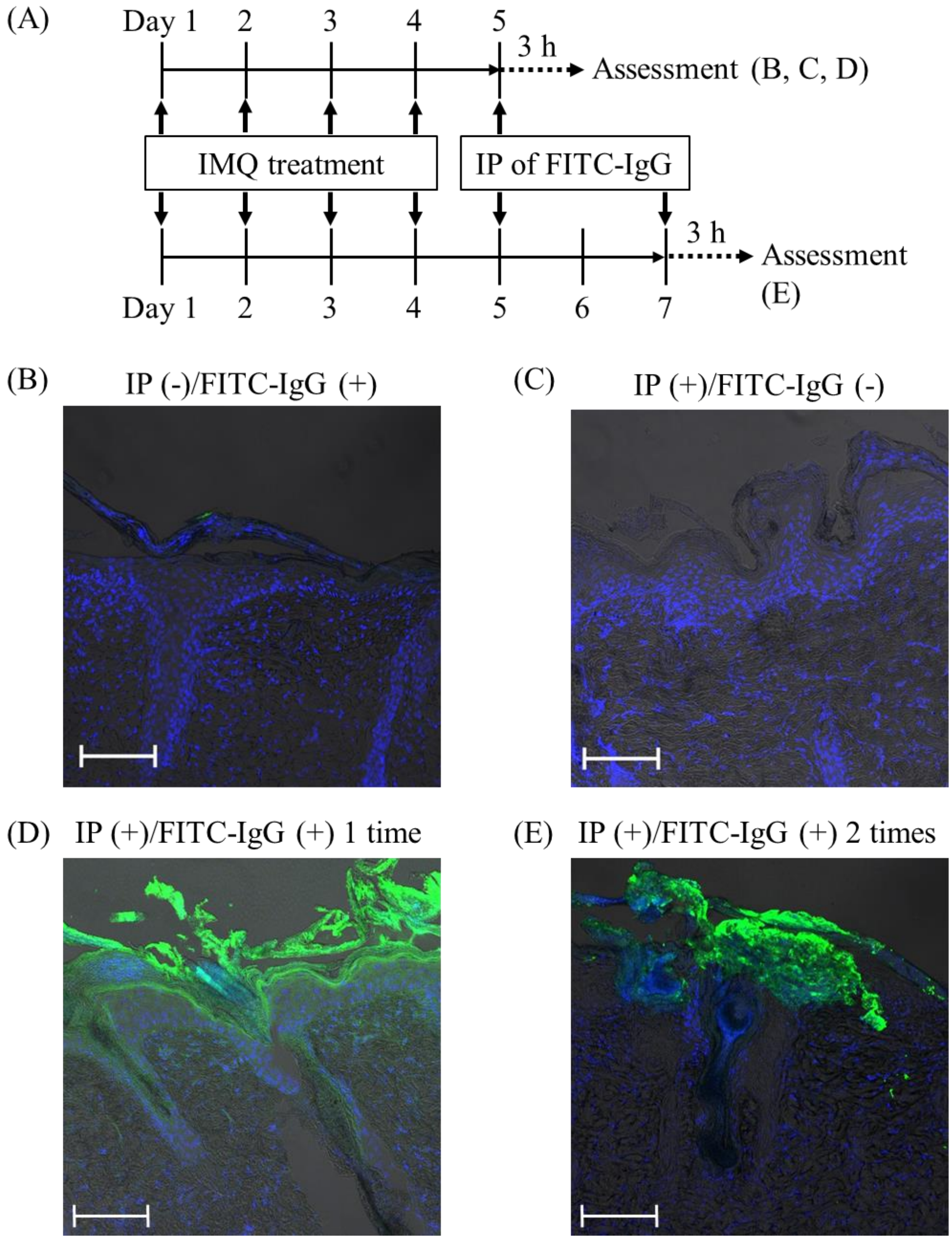

Fig. 4. Iontophoretic delivery of fluorescent-labeled antibody into the dorsal skin of IMQ-induced psoriasis model rats.

Experimental schedule (A). Twenty-four hours (day 5) after the 4th IMQ treatment (day 4), the rats were treated with FITC-IgG alone (B; n=3), IP alone (C; n=3), or IP administration of FITC-IgG (D; n=3), followed by preparation of 10-µm frozen skin sections 3 h after treatment. In those rats administered FITC-IgG by IP twice (E; n=3, day 5 and 7), the sections were prepared 3 h after the 2nd treatment. Confocal images of each group are shown (B; IP (-)/FITC-IgG (+), C; IP (+)/FITC-IgG (-), D; IP (+)/FITC-IgG (+) 1 time, E; IP (+)/FITC-IgG (+) 2 times). Merged images of phase contrast, DAPI (nuclei; blue), and FITC (IgG; green) are shown. Scale bars = 100 µm.

3.3. Iontophoretic delivery of etanercept

Next, we examined the biological function of a macromolecular drug delivered into the psoriatic skin via IP. The anti-TNF-α drug etanercept was chosen as a representative therapeutic biological macromolecular drug in this study. Since there are a lot of reports about the usefulness of etanercept on several inflammatory diseases such as psoriasis in mice [25], arthritis [26, 27], and traumatic brain injury in rats [28], cross reactivity of etanercept between human and rats has been demonstrated. IP treatments (0.4 mA/cm^2, 1 h) of etanercept were performed on the psoriatic inflamed skin at 24 and 72 h after the last IMQ treatment, followed by assessment of mRNA levels of inflammatory cytokines (TNF-α and IL-6), as shown in Fig. 5A. The results showed that mRNA levels of TNF-α and IL-6 were significantly increased in IMQ-treated psoriasis model rats compared with normal rats (IMQ (-)) (Figs. 5B and C). As several inflammatory cytokines have been reported to induce hyperplasia of the epidermis, these results provide support for the HE staining image of the psoriatic dorsal skin shown in Figure 3. Transdermal administration of etanercept via IP had no effect on TNF-α mRNA levels in comparison with non-treated and PBS (IP) groups (Fig. 5D). On the other hand, IL-6 mRNA levels were significantly reduced by IP delivery of etanercept compared with non-treated and PBS (IP)-treated groups (Fig. 5E). By performing Western blotting, we also evaluated TNF-α protein expression in psoriatic skin and effect of IP-mediated delivered etanercept on its expression. The results showed that IMQ treatment markedly increased TNF-α protein expression compared with normal rat (Supplementary Fig. 1A). The levels of TNF-α protein expression was significantly decreased by etanercept administration via IP compared with IMQ-treated rats (Supplementary Fig. 1A and B), although decrease of the expression was only 14% at day 8 of the present therapeutic regimen. It is previously reported that TNF-α induces upregulation of IL-6 mRNA via NF-κB phosphorylation in skin cells under inflammatory conditions [29, 30]. Based on these reports and our present results, it is suggested that etanercept exerts its function upon delivery into psoriatic skin via IP and captures TNF-α, resulting in possible suppression of downstream signaling and decrease of upregulated IL-6 mRNA; although upregulation of TNF-α mRNA could not be inhibited by etanercept.

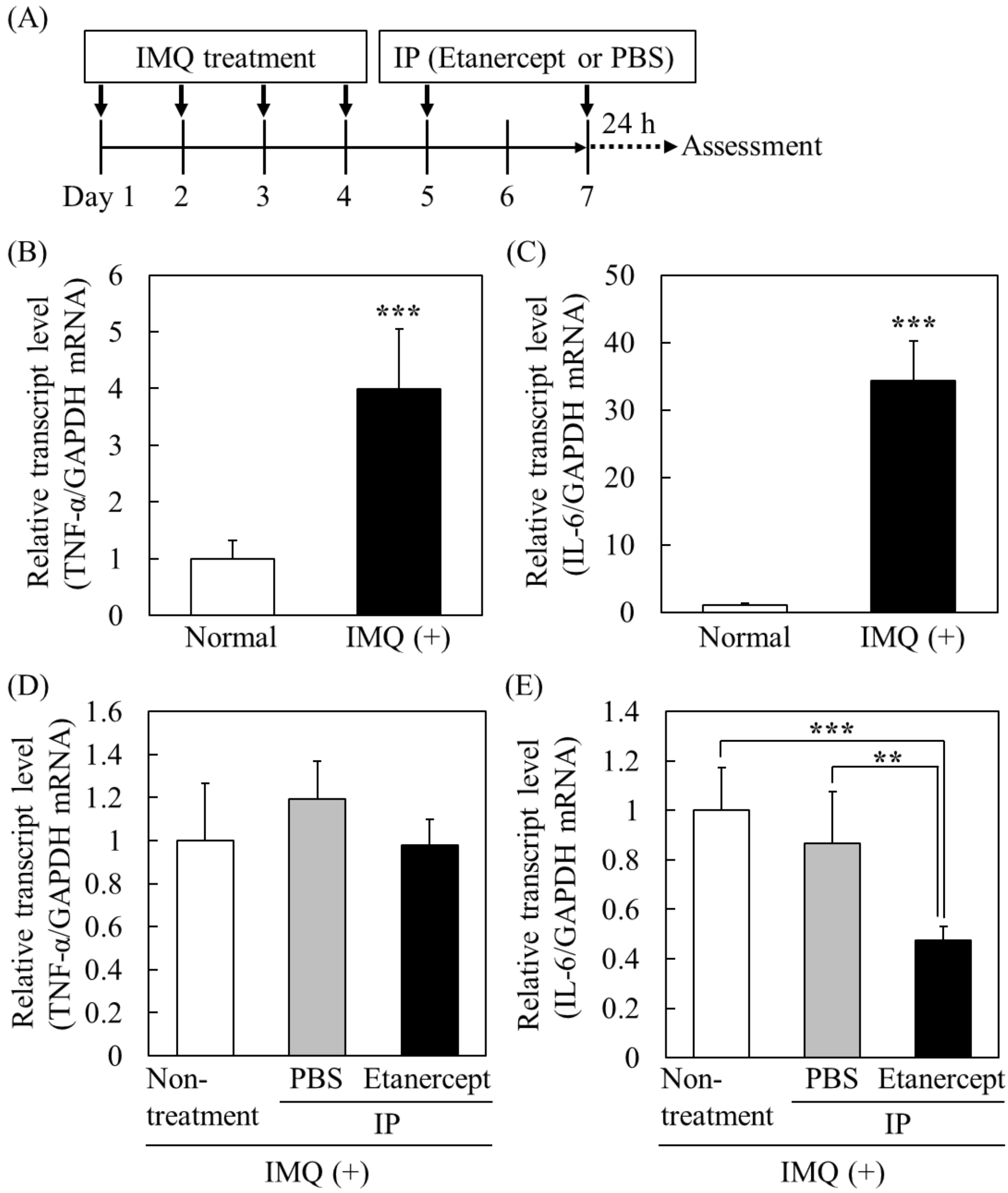

Fig. 5. Effects of IP-mediated etanercept treatment on inflammatory cytokine mRNA levels in psoriasis model rats.

IMQ-treated psoriasis model rats were transdermally administered etanercept (1 mg dose/rat) or PBS via IP 5 and 7 days after the start of IMQ treatment (A). Eight days after the start of IMQ treatment, the mRNA levels of TNF-α (B) and IL-6 (C) were assessed. The relative transcript levels of TNF-α and IL-6 in IMQ (+) to those in the IMQ (-) non-treated group are presented. In the IP-treated group, the mRNA levels of TNF-α (D) and IL-6 (E) were assessed at 24 h after the 2nd IP treatment. The relative transcript levels in each group to those in the IMQ (+) non-treated group are presented. Data are mean ± S.D. (n=4). ** *P*<0.01, *** *P*<0.001.

3.4. Effect of subcutaneous injection of etanercept into psoriasis model rats

Following the successful demonstration that biological macromolecular drugs can be delivered into skin tissue by IP and exert their native functions, we compared IP with a conventional administration route of etanercept for psoriasis treatment, namely *s.c.* injection. The experimental procedure for *s.c.* injection was similar to that of IP administration with the exception that etanercept and PBS were injected *s.c.* into the psoriasis model rats (Fig. 6A). In the *s.c.* PBS-treated group, TNF-α mRNA levels tended to increase, and a significant increase of IL-6 mRNA levels was induced (Fig. 6B and C), suggesting that needle insertion into psoriatic skin causes an inflammatory reaction. In contrast, in the groups receiving *s.c.* injection of etanercept into lesion or non-lesion sites, mRNA levels of TNF-α and IL-6 tended to be lower than those of PBS-treated groups, whereas levels were comparable to or higher than those of the IMQ (+) group (Figs. 6B and C). The results shown in Figs. 5 and 6 demonstrate that IP can more effectively deliver biological macromolecular drugs into inflamed skin without induction of an inflammatory reaction as induced by conventional *s.c.* injection with needle. In addition, as shown in the images of HE staining in Supplementary Fig. 2, *s.c.* needle insertion caused scars of needle penetration from epidermis to dermis layers both in normal and psoriatic skins. On the other hand, IP treatment hardly caused such scars and obvious damage including epidermis hyperplasia by inflammation in the skin tissues, suggesting that IP is non-invasive delivery method without induction of obvious skin damage compared with *s.c.* injection.

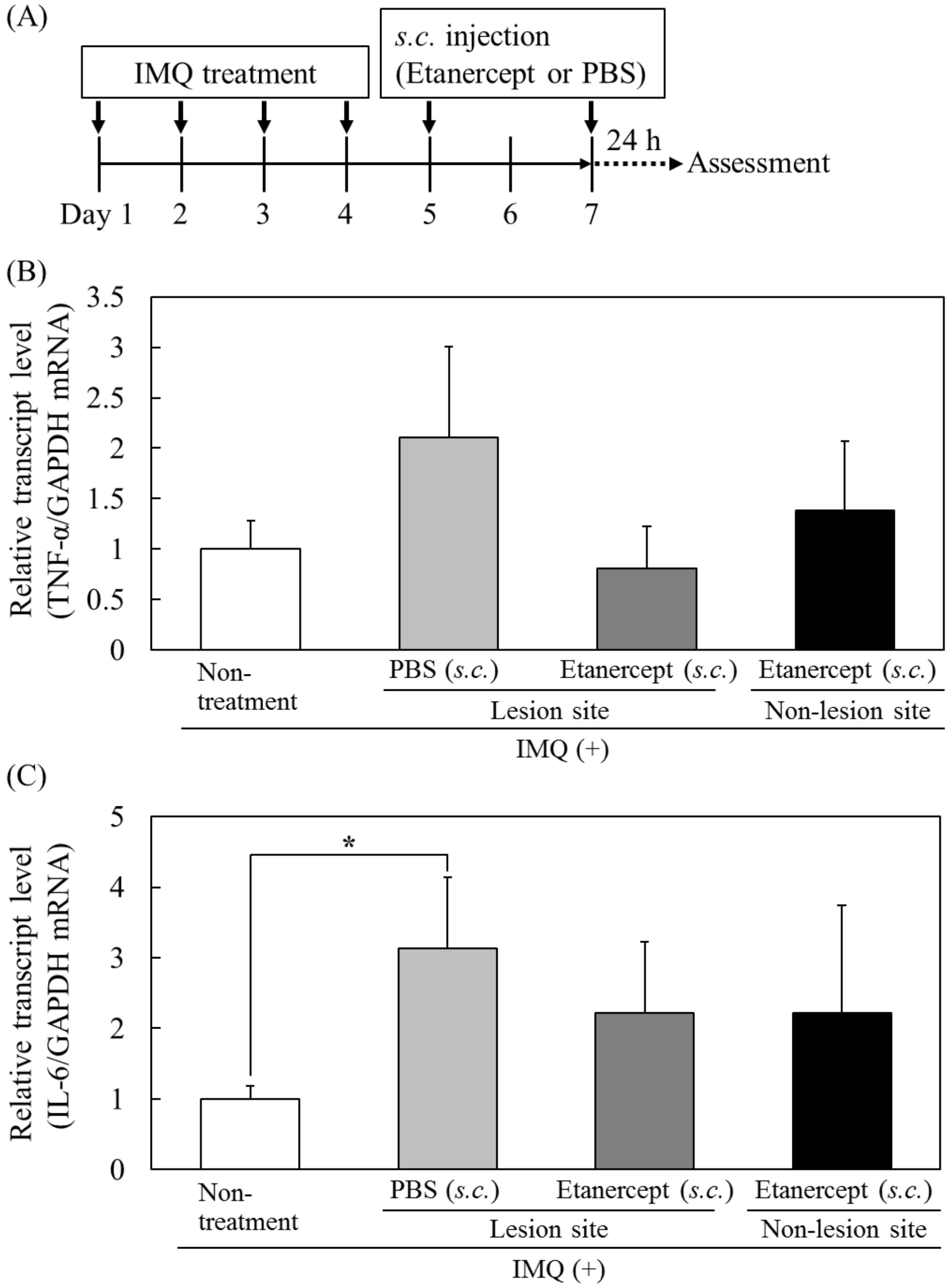

Fig. 6. Effects of subcutaneous (*s.c.*) injection of etanercept on inflammatory cytokine mRNA levels in the psoriasis model rats.

IMQ-treated psoriasis model rats were subcutaneously injected with etanercept (1 mg dose/rat) or PBS at 5 and 7 days after the start of IMQ treatment (A). In etanercept-treated groups, *s.c.* injections were performed directly into the psoriatic inflammatory skin (lesion site) or the distal area from the diseased site (non-lesion site), respectively. Twenty-four hours after the 2nd *s.c.* injection, the mRNA levels of TNF-α (B) and IL-6 (C) were evaluated. The relative transcript levels of TNF-α and IL-6 in each group to those in the IMQ (+) group are presented. Data are mean ± S.D. (n=3). * $P<0.05$.

3.5. Therapeutic outcome of etanercept delivered via IP on psoriasis

Finally, we investigated therapeutic outcome of etanercept delivered via IP in psoriasis model rats by evaluating epidermis thickness as an indication of epidermis hyperplasia. The results of HE staining showed that the IMQ treatment significantly induced epidermis hyperplasia compared with non-treated normal hairless rats (Figs. 7A, B, and E), similar to the images of HE staining in Fig. 3. IP administration of etanercept significantly ameliorated epidermis hyperplasia in comparison to IMQ-treated rats (Figs. 7C and E). Importantly, the therapeutic effect of IP-delivered etanercept was significantly higher than *s.c.* injected etanercept (Figs. 7C-E). These results suggest that etanercept delivered by IP effectively exerted its function and ameliorated the symptom of psoriasis in IMQ-treated model rats, and that IP should be useful as a non-invasive transdermal delivery technology of biological macromolecular drugs, such as antibodies and fusion proteins.

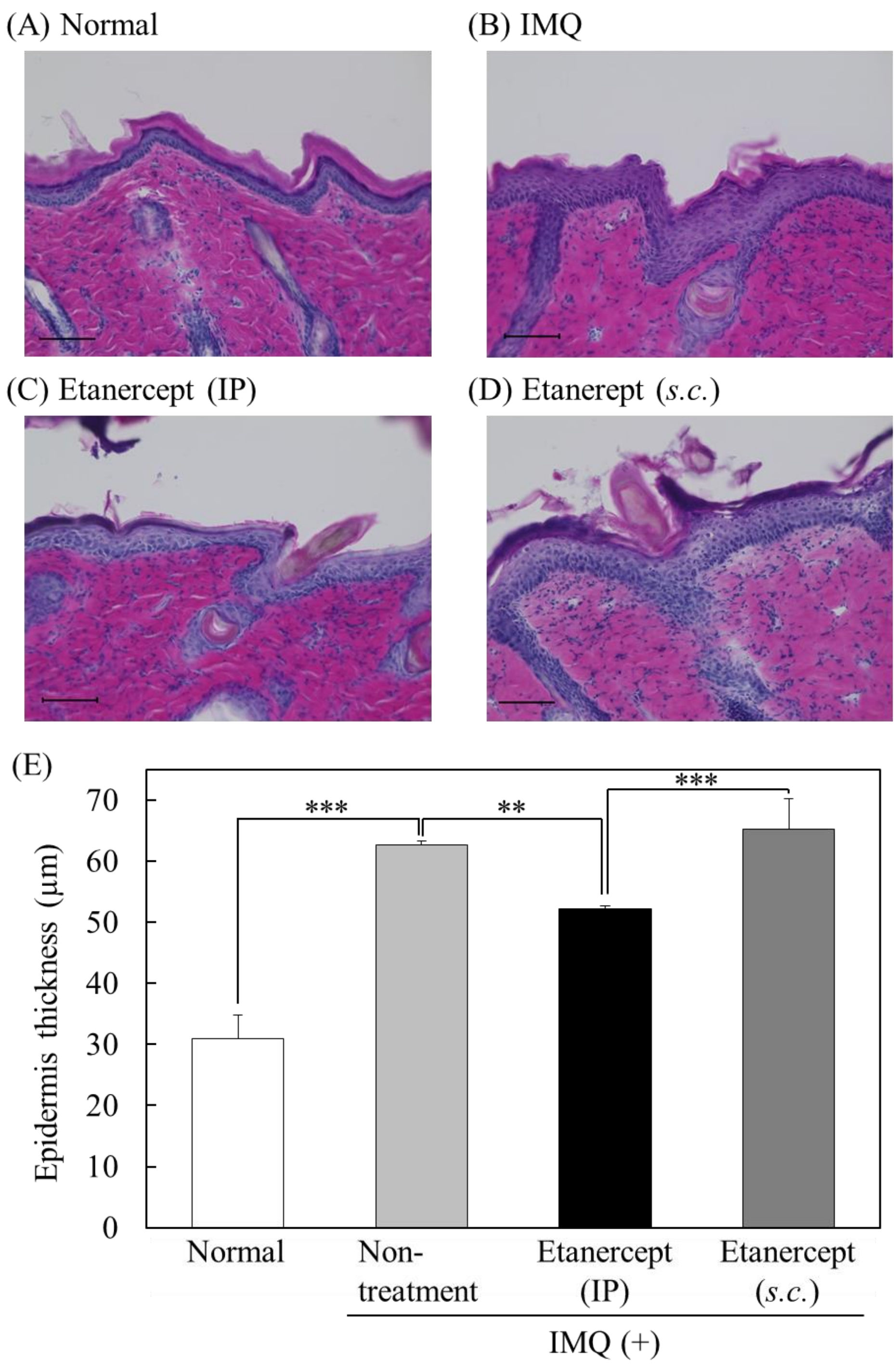

Fig. 7. Amelioration of epidermis hyperplasia by etanercept delivered via IP in psoriasis model rats.

Etanercept (1 mg dose/rat) was transdermally (IP) or subcutaneously administered 5 and 7 days after the start of IMQ treatment. Eight days after the start of IMQ treatment, the 10-µm frozen skin sections were prepared and stained with HE. Microscopic images of skin sections from normal (A; n=3), IMQ-treated psoriasis model rats (B; n=4), the model rats treated with etanercept administered by IP (C; n=4) or *s.c.* injection (D; n=4). Scale bars = 100 µm. From the images of HE-stained skin sections, epidermis thickness of each group of rats was measured (E). Data are mean ± S.D. (n=4). ** P<0.01, *** P<0.001.

4. Discussion

Our previous studies revealed that hydrophilic macromolecules, such as siRNA and CpG oligo DNA as well as nanoparticles including liposomes and nanogels, can be intradermally delivered into skin tissue by intercellular junction cleavage via IP using weak electric current (0.3-0.5 mA/cm^2) [18-21]. We also demonstrated that activation of protein kinase C-α and Ca^{2+} influx is involved in the intercellular junction cleavage via gap junction dissociation by Cx43 reduction and filamentous actin depolymerization [22]. Based on these findings, we sought to apply IP to the intradermal delivery of biological macromolecular drugs, including antibodies. As shown in Fig. 1, FITC-IgG permeated into the skin tissue around the epidermis immediately after 1-h IP (Fig. 1C), although passive diffusion was not observed. By quantification of the retained FITC-IgG in nonwoven fabric immediately after IP, it was revealed that approximately 80% of the FITC-IgG could be administered by IP, although the intradermal amount of FITC-IgG could not be detected. Broad FITC fluorescence of the antibody was observed both in and around the epidermis and dermis layers at 3 h after IP administration (Figs. 1D and E). In particular, the fluorescence of FITC-IgG was remarkably observed in the region where the expression of intercellular gap junction protein Cx43 decreased via IP (Fig. 2). These results suggest that antibodies that exhibit higher molecular weights compared with functional nucleic acids, including siRNA, can also reach the dermis layer from the epidermis layer via the cleaved cellular gap due to IP.

We applied the IP delivery technology to the treatment of psoriasis. In IMQ-induced psoriasis model rats, FITC-IgG administered via IP was found to permeate into inflamed skin tissue (Figs. 4D and E). However, in the psoriasis model, the IP-delivered antibodies only reached shallow sites compared with normal skin tissue (Figs. 1C-E). It was previously reported that keratinocytes in the epidermis are highly proliferative in response to several inflammatory cytokines, including TNF-α and IL-6, in inflamed psoriatic skin [29, 31, 32]. Indeed, hyperplasia of epidermis was clearly observed in the dorsal skin of hairless rats after IMQ treatment in the present study (Fig. 3). The proliferating keratinocytes secrete various cytokines to migrate immune cells such as leukocytes and

T cells into the layers of epidermis and dermis [33]. Based on these findings, it is considered that the psoriatic skin forms cellular barriers due to the epidermis hyperplasia by over-proliferated keratinocytes and accumulated immune cells. Owing to the cellular barriers in the skin, the effect of intercellular junction cleavage via IP would not have reached the dermis layer of psoriatic skin, so that the FITC-IgG administered by IP could not penetrate so deeply into the psoriatic skin and might stay in the stratum corneum and epidermis layer in the confocal images (Fig. 4).

The function of intradermally-delivered biological macromolecular drugs was evaluated using the anti-TNF-α drug etanercept as a representative therapeutic agent. It was previously reported that under psoriatic conditions, TNF-α produced in the skin immune cells and keratinocytes binds to its receptors and activates the NF-κB signaling pathway, resulting in promotion of IL-6 production [29, 30, 32]. In the present study, IMQ treatment onto the dorsal skin of rats significantly induced upregulation of both TNF-α and IL-6 mRNA levels (Fig. 5). Only IP treatment had minimal effects on mRNA levels. IP administration of two doses of etanercept significantly reduced IL-6 mRNA levels by 50%, whereas levels of TNF-α mRNA were not reduced by etanercept IP. On the other hand, the expression of TNF-α protein in the psoriatic skins significantly decreased by IP-mediated delivery of etanercept (Supplementary Fig. 1), although decrease of the expression was only 14% at day 8 of the present therapeutic regimen. These results suggest that etnercept was efficiently delivered into psoriatic skin by IP and exerted its function, capturing TNF-α around the diseased sites, and possibly resulting in subsequent inhibition of downstream inflammatory signals.

Needle injection into inflamed skin can cause further progression of inflammation [11, 34]. In fact, in the present study, *s.c.* needle injection into the dorsal skin of IMQ-treated rats induced an increase in both TNF-α and IL-6 levels (Fig. 6). On the other hand, when etanercept was administered via *s.c.* injection, the mRNA levels of these inflammatory cytokines did not decrease compared with the IMQ-treated group, regardless of whether the injection was performed on lesion or non-lesion sites. However, *s.c.* injection of etanercept tended to decrease the levels compared with those of the PBS group. These results suggest that while *s.c.*-injected etanercept was able to exert its effect, the effect was offset by the invasiveness of the needle injection. In fact, *s.c.* needle insertion caused scars of needle penetration from epidermis to dermis layers both in normal and psoriatic skins, whereas IP treatment hardly caused such scars and obvious damage including epidermis hyperplasia by inflammation in the skin tissues (Supplementary Fig. 2). The exact reason for increase of IL-6 mRNA in the group of *s.c.* injection of etanercept is unclear. However, various inflammatory cytokines and signal pathways including NF-κB and signal transducer and activator of transcription (STAT) are intricately involved in pathological progression of psoriasis [33]. The reason that IL-6 mRNA increased about 2-fold is considered that *s.c.* injection induced production of several cytokines around the psoriasis sites via needle-induced skin surface bleeding, tissue cut, bruising, and blood vessel breakage [35]. Then, the inflammatory pathways including NF-κB and STAT were activated, resulting in increase of downstream IL-6 mRNA expression. The reason why the mRNA levels of TNF-α and IL-6 tended to be elevated by *s.c.* injection of etanercept in the non-lesion sites is also unclear. It has been reported that psoriasis is recognized as a chronic and immune-mediated disease involved in systemic inflammation [36, 37]. It is presumed that, by needle insertion into the non-psoriatic lesion site, inflammation reaction was promoted around the injection site, resulting in increase of the mRNA levels of TNF-α and IL-6 around the non-lesion site. On the other hand, intradermal administration of etanercept via IP significantly reduced IL-6 mRNA levels without induction of further inflammation into psoriatic skin. Moreover, etanercept delivered via IP showed significantly higher therapeutic effect on epidermis hyperplasia induced by psoriasis than *s.c.* injected etanercapt (Fig. 7). An advantage of IP over *s.c.* injection is that *s.c.*-injected drug solution rapidly diffuses in skin tissue, whereas IP-administered drugs can permeate evenly into the skin. In addition, it has also been reported that drugs that permeate into the skin tissue via IP gradually move into the bloodstream via the skin acting as a drug reservoir [12, 20]. Taken together, these findings suggest that IP should be useful as a non-invasive and efficient intradermal delivery technology of biological macromolecular drugs, without causing an inflammatory reaction.

We recently reported that weak electric current treatment for IP can deliver hydrophilic macromolecules, such as siRNA and antibodies, into the cytoplasm by inducing endocytosis with unique properties *in vitro* [38-40]. The resultant endosomes induced by this unique endocytosis process have been suggested to allow macromolecules (M.W. less than ca. 70,000) to leak through ceramide pores formed in the endosomal membranes [41]. In the case of cytoplasmic delivery of antibodies (M.W. 150,000) into cultured cells, we combined weak current treatment with chloroquine, which is an endosome disrupting agent, to overcome the limitation of high molecular weight macromolecules not being able to escape from endosomes. In this study, biological macromolecular drugs were successfully delivered into skin tissue and shown to subsequently capture target inflammatory cytokines, resulting in psoriasis-induced IL-6 upregulation. It is speculated that some of the intradermally delivered macromolecular drugs by IP were taken up into the skin cells; although such molecules likely cannot escape from the endosomes. Thus, by modification of biological macromolecular drugs with certain elements that promote endosomal escape, it should be possible to capture intracellular target molecules involved in pathological progression of diseases, as well as extracellular molecules (e.g., inflammatory cytokines) by using an IP-mediated delivery system. Design and IP-mediated delivery of such functional macromolecular drugs should be useful and interesting for future studies.

In the present study, intradermal delivery of biological macromolecular drugs with retained functionality was achieved by IP. High costs and frequent administration are generally associated with treatments that involve biological macromolecular drugs, which proves to be an economic burden for patients [6]. As shown in Figs. 5 and 6, IP-mediated delivery demonstrated a superior effect of etanercept on inflammatory signals induced by psoriasis, compared with the effect of *s.c.* injection, resulting in significantly higher therapeutic effect on epidermis hyperplasia in the group of etanercept delivered via IP (Fig. 7). Thus, non-invasive and efficient drug delivery by IP is expected to improve quality of life for patients. Although we could observe intradermal permeation of FITC-IgG and therapeutic effect of IP-delivered etanercept in this study, determination of the amount of biological macromolecular drugs in the skin tissues could not be achieved. Hence, establishment of a method for quantifying the intradermally delivered drugs is important issue in future study. We also previously succeeded in treating diabetes by IP of insulin-encapsulated liposomes [20], cancer immunotherapy by IP delivery of antigen-possessing nanogels [21] or CpG-oligo DNA [19], and suppression of upregulation of specific mRNA in atopic skin [18]. The results of both our past and present studies suggest that an intradermal drug delivery system using IP offers the potential to be applied to diverse therapeutic agents for the treatment of various diseases.

5. Conclusions

In summary, the present study demonstrated that non-invasive and efficient intradermal delivery of antibodies was achieved by IP using weak electric current (0.4 mA/cm^2). Transdermally delivered antibodies extended from the epidermis layer to the dermis layer. We also demonstrated the successful IP-mediated delivery of antibodies into psoriatic inflamed skin tissue in IMQ-treated psoriasis model rats. In addition, upregulation of mRNA levels of IL-6, which is involved in pathological progression of psoriasis, was significantly suppressed by IP of etanercept (anti-TNF-α drug: recombinant human TNF-α receptor), while levels were not suppressed following *s.c.* injection. Importantly, IP administration of etanercept significantly ameliorated epidermis hyperplasia in IMQ-treated psoriasis model rats, and the effect was significantly higher than *s.c.* injected etanercept. Taken together, these results suggest that IP can be applied as a non-invasive and efficient intradermal drug delivery technology for biological macromolecular drugs, such as antibodies and anti-cytokine therapeutics. To the best of our knowledge, this is the first report of intradermal delivery of biological macromolecular drugs via IP.

Acknowledgements

This research was supported by the Research Program for the Development of Intelligent Tokushima Artificial Exosome (iTEX) from Tokushima University.

Declaration of interest statement

The authors declare no competing financial interests.

References

[1] P.J. Carter, G.A. Lazar, Next generation antibody drugs: pursuit of the 'high-hanging fruit', Nat Rev Drug Discov, 17 (2018) 197-223.

[2] K. Imai, A. Takaoka, Comparing antibody and small-molecule therapies for cancer, Nat Rev Cancer, 6 (2006) 714-727.

[3] A. Beck, T. Wurch, C. Bailly, N. Corvaia, Strategies and challenges for the next generation of therapeutic antibodies, Nat Rev Immunol, 10 (2010) 345-352.

[4] H.S. Gill, M.R. Prausnitz, Does needle size matter?, J Diabetes Sci Technol, 1 (2007) 725-729.

[5] J.J. Norman, M.R. Prausnitz, Improving patient acceptance of insulin therapy by improving needle design, J Diabetes Sci Technol, 6 (2012) 336-338.

[6] M. Miller, E. Pisani, The cost of unsafe injections, Bull World Health Organ, 77 (1999) 808.

[7] Y. Deng, C. Chang, Q. Lu, The Inflammatory Response in Psoriasis: a Comprehensive Review, Clin Rev Allergy Immunol, 50 (2016) 377-389.

[8] J.E. Hawkes, T.C. Chan, J.G. Krueger, Psoriasis pathogenesis and the development of novel targeted immune therapies, J Allergy Clin Immunol, 140 (2017) 645-653.

[9] A.C. Chan, P.J. Carter, Therapeutic antibodies for autoimmunity and inflammation, Nat Rev Immunol, 10 (2010) 301-316.

[10] P.J. Mease, B.S. Goffe, J. Metz, A. VanderStoep, B. Finck, D.J. Burge, Etanercept in the treatment of psoriatic arthritis and psoriasis: a randomised trial, Lancet, 356 (2000) 385-390.

[11] M. Abrouk, M. Nakamura, T.H. Zhu, B. Farahnik, R.K. Singh, K.M. Lee, M.V. Jose, J. Koo, T. Bhutani, W. Liao, The Patient's Guide to Psoriasis Treatment. Part 3: Biologic Injectables, Dermatol Ther (Heidelb), 6 (2016) 325-331.

[12] Y.N. Kalia, A. Naik, J. Garrison, R.H. Guy, Iontophoretic drug delivery, Adv Drug Deliv Rev, 56 (2004) 619-658.

[13] R.H. Guy, Y.N. Kalia, M.B. Delgado-Charro, V. Merino, A. López, D. Marro, Iontophoresis: electrorepulsion and electroosmosis, J Control Release, 64 (2000) 129-132.

[14] A.R. Denet, R. Vanbever, V. Preat, Skin electroporation for transdermal and topical delivery, Adv Drug Deliv Rev, 56 (2004) 659-674.

[15] S. Mitragotri, D. Blankschtein, R. Langer, Transdermal drug delivery using low-frequency sonophoresis, Pharm Res, 13 (1996) 411-420.

[16] H. Du, P. Liu, J. Zhu, J. Lan, Y. Li, L. Zhang, J. Zhu, J. Tao, Hyaluronic Acid-Based Dissolving Microneedle Patch Loaded with Methotrexate for Improved Treatment of Psoriasis, ACS Appl Mater Interfaces, 11 (2019) 43588-43598.

[17] M.R. Prausnitz, R. Langer, Transdermal drug delivery, Nat Biotechnol, 26 (2008) 1261-1268.

[18] K. Kigasawa, K. Kajimoto, S. Hama, A. Saito, K. Kanamura, K. Kogure, Noninvasive delivery of siRNA into the epidermis by iontophoresis using an atopic dermatitis-like model rat, Int J Pharm, 383 (2010) 157-160.

[19] K. Kigasawa, K. Kajimoto, T. Nakamura, S. Hama, K. Kanamura, H. Harashima, K. Kogure, Noninvasive and efficient transdermal delivery of CpG-oligodeoxynucleotide for cancer immunotherapy, J Control Release, 150 (2011) 256-265.

[20] K. Kajimoto, M. Yamamoto, M. Watanabe, K. Kigasawa, K. Kanamura, H. Harashima, K. Kogure, Noninvasive and persistent transfollicular drug delivery system using a combination of liposomes and iontophoresis, Int J Pharm, 403 (2011) 57-65.

[21] M. Toyoda, S. Hama, Y. Ikeda, Y. Nagasaki, K. Kogure, Anti-cancer vaccination by transdermal delivery of antigen peptide-loaded nanogels via iontophoresis, Int J Pharm, 483 (2015) 110-114.

[22] S. Hama, Y. Kimura, A. Mikami, K. Shiota, M. Toyoda, A. Tamura, Y. Nagasaki, K. Kanamura, K. Kajimoto, K. Kogure, Electric Stimulus Opens Intercellular Spaces in Skin, J Biol Chem, 289 (2014) 2450-2456.

[23] K. Satake, T. Amano, T. Okamoto, Low systemic exposure and calcemic effect of calcipotriol/betamethasone ointment in rats with imiquimod-induced psoriasis-like dermatitis, Eur J Pharmacol, 826 (2018) 31-38.

[24] A. Ueyama, M. Yamamoto, K. Tsujii, Y. Furue, C. Imura, M. Shichijo, K. Yasui, Mechanism of

pathogenesis of imiquimod-induced skin inflammation in the mouse: a role for interferon-alpha in dendritic cell activation by imiquimod, J Dermatol, 41 (2014) 135-143.

[25] Z. Liu, H. Liu, P. Xu, Q. Yin, Y. Wang, Y.K. Opoku, J. Yang, L. Song, X. Sun, T. Zhang, D. Yu, X. Wang, G. Ren, D. Li, Ameliorative effects of a fusion protein dual targeting interleukin 17A and tumor necrosis factor alpha on imiquimod-induced psoriasis in mice, Biomed Pharmacother, 108 (2018) 1425-1434.

[26] P. Totoson, K. Maguin-Gate, A. Prigent-Tessier, A. Monnier, F. Verhoeven, C. Marie, D. Wendling, C. Demougeot, Etanercept improves endothelial function via pleiotropic effects in rat adjuvant-induced arthritis, Rheumatology (Oxford), 55 (2016) 1308-1317.

[27] Q.T. Wang, Y.J. Wu, B. Huang, Y.K. Ma, S.S. Song, L.L. Zhang, J.Y. Chen, H.X. Wu, W.Y. Sun, W. Wei, Etanercept attenuates collagen-induced arthritis by modulating the association between BAFFR expression and the production of splenic memory B cells, Pharmacol Res, 68 (2013) 38-45.

[28] C.-C. Chio, C.-H. Chang, C.-C. Wang, C.-U. Cheong, C.-M. Chao, B.-C. Cheng, C.-Z. Yang, C.-P. Chang, Etanercept attenuates traumatic brain injury in rats by reducing early microglial expression of tumor necrosis factor-α, BMC Neurosci, 14 (2013) 33.

[29] H. Chen, C. Lu, H. Liu, M. Wang, H. Zhao, Y. Yan, L. Han, Quercetin ameliorates imiquimod-induced psoriasis-like skin inflammation in mice via the NF-kappaB pathway, Int Immunopharmacol, 48 (2017) 110-117.

[30] J.-W. Cho, K.-S. Lee, C.-W. Kim, Curcumin attenuates the expression of IL-1β, IL-6, and TNF-α as well as cyclin E in TNF-α-treated HaCaT cells; NF-κB and MAPKs as potential upstream targets, Int J Mol Med, 19 (2007) 469-474.

[31] R. Dou, Z. Liu, X. Yuan, D. Xiangfei, R. Bai, Z. Bi, P. Yang, Y. Yang, Y. Dong, W. Su, D. Li, C. Mao, PAMs ameliorates the imiquimod-induced psoriasis-like skin disease in mice by inhibition of translocation of NF-kappaB and production of inflammatory cytokines, PLoS One, 12 (2017) e0176823.

[32] F. Fantuzzi, M. Del Giglio, P. Gisondi, G. Girolomoni, Targeting tumor necrosis factor α in

psoriasis and psoriatic arthritis, Expert Opin Ther Targets, 12 (2008) 1085-1096.

[33] M.A. Lowes, A.M. Bowcock, J.G. Krueger, Pathogenesis and therapy of psoriasis, Nature, 445 (2007) 866-873.

[34] X. Guo, W. Wang, Challenges and recent advances in the subcutaneous delivery of insulin, Expert Opin Ther Targets, 14 (2017) 727-734.

[35] P. Crocker, K. Maynard, M. Little, Pain free blunt needle injection technology, Innov Pharmaceut technol, 9 (2001) 111-115.

[36] K. Reich, The concept of psoriasis as a systemic inflammation: implications for disease management, J Eur Acad Dermatol Venereol, 26 Suppl 2 (2012) 3-11.

[37] E.A. Dowlatshahi, E.A. van der Voort, L.R. Arends, T. Nijsten, Markers of systemic inflammation in psoriasis: a systematic review and meta-analysis, Br J Dermatol, 169 (2013) 266-282.

[38] M. Hasan, A. Nishimoto, T. Ohgita, S. Hama, H. Kashida, H. Asanuma, K. Kogure, Faint electric treatment-induced rapid and efficient delivery of extraneous hydrophilic molecules into the cytoplasm, J Control Release, 228 (2016) 20-25.

[39] M. Hasan, N. Tarashima, K. Fujikawa, T. Ohgita, S. Hama, T. Tanaka, H. Saito, N. Minakawa, K. Kogure, The novel functional nucleic acid iRed effectively regulates target genes following cytoplasmic delivery by faint electric treatment, Sci Technol Adv Mater, 17 (2016) 554-562.

[40] M. Hasan, S. Hama, K. Kogure, Low Electric Treatment activates Rho GTPase via Heat Shock Protein 90 and Protein Kinase C for Intracellular Delivery of siRNA, Sci Rep, 9 (2019).

[41] T. Torao, M. Mimura, Y. Oshima, K. Fujikawa, M. Hasan, T. Shimokawa, N. Yamazaki, H. Ando, T. Ishida, T. Fukuta, T. Tanaka, K. Kogure, Characteristics of unique endocytosis induced by weak current for cytoplasmic drug delivery, Int J Pharm, 576 (2020) 119010.

Figure legends

Fig. 1. Intradermal distribution of fluorescent-labeled antibody delivered by iontophoresis (IP).

Confocal images of 10-μm frozen skin sections of hairless rats applied with FITC-IgG without IP (0.4 mA/cm2) for 3 h (A; n=3) and 3 h after treatment by 1-h IP alone (B; n=3). The hairless rats were also transdermally administered FITC-IgG via 1-h IP. At 0 h (C; n=4) and 3 h (D and E; n=4) after 1-h IP, FITC fluorescence was observed by confocal microscopy. Scale bars = 100 μm. Image of dorsal skin tissue of hairless rats stained with HE (F). Stratum corneum, epidermis, and dermis. Scale bar = 100 μm.

Fig. 2. Transdermal permeation of fluorescence-labeled antibody via the cleaved intercellular junctions induced by IP.

The rats were transdermally administered FITC-IgG via 1-h IP. Three hours after 1-h IP, the skins of the rats were dissected, and 10-μm frozen sections were prepared, followed by immunostaining for an intercellular gap junction protein Cx43. The fluorescence images of the skin were obtained by confocal laser scanning microscopy. The images of the skin sections (A; IP (-)), (B; IP (+)/FITC-IgG (-), (C) IP (+)/FITC-IgG (+)) are shown. (C) The images in left column indicate the images obtained around the epidermis and those in right column around the dermis. Green and red indicate FITC (IgG) and Alexa647 (Cx43), respectively. Merged images of FITC, Alexa647, and blight field are shown. Scale bars = 50 μm. The experiments were independently performed three times.

Fig. 3. Evaluation of psoriatic skin inflammation in IMQ-induced psoriasis model rats.

The psoriasis model rats were prepared by topical application of IMQ cream (60 mg/rat/treatment) a total of four times. Eight days after the 1st IMQ treatment (day 1), 10-μm frozen skin sections were prepared, and HE staining was performed. Microscopic images of skin sections from normal (A) and IMQ-treated psoriasis model rats (B). Scale bars = 100 µm.

Fig. 4. Iontophoretic delivery of fluorescent-labeled antibody into the dorsal skin of IMQ-induced psoriasis model rats.

Experimental schedule (A). Twenty-four hours (day 5) after the 4th IMQ treatment (day 4), the rats were treated with FITC-IgG alone (B; n=3), IP alone (C; n=3), or IP administration of FITC-IgG (D; n=3), followed by preparation of 10-µm frozen skin sections 3 h after treatment. In those rats administered FITC-IgG by IP twice (E; n=3, day 5 and 7), the sections were prepared 3 h after the 2nd treatment. Confocal images of each group are shown (B; IP (-)/FITC-IgG (+), C; IP (+)/FITC-IgG (-), D; IP (+)/FITC-IgG (+) 1 time, E; IP (+)/FITC-IgG (+) 2 times). Merged images of phase contrast, DAPI (nuclei; blue), and FITC (IgG; green) are shown. Scale bars = 100 µm.

Fig. 5. Effects of IP-mediated etanercept treatment on inflammatory cytokine mRNA levels in psoriasis model rats.

IMQ-treated psoriasis model rats were transdermally administered etanercept (1 mg dose/rat) or PBS via IP 5 and 7 days after the start of IMQ treatment (A). Eight days after the start of IMQ treatment, the mRNA levels of TNF-α (B) and IL-6 (C) were assessed. The relative transcript levels of TNF-α and IL-6 in IMQ (+) to those in the IMQ (-) non-treated group are presented. In the IP-treated group, the mRNA levels of TNF-α (D) and IL-6 (E) were assessed at 24 h after the 2nd IP treatment. The relative transcript levels in each group to those in the IMQ (+) non-treated group are presented. Data are mean ± S.D. (n=4). ** P<0.01, *** P<0.001.

Fig. 6. Effects of subcutaneous (*s.c.*) injection of etanercept on inflammatory cytokine mRNA levels in the psoriasis model rats.

IMQ-treated psoriasis model rats were subcutaneously injected with etanercept (1 mg dose/rat) or PBS at 5 and 7 days after the start of IMQ treatment (A). In etanercept-treated groups, *s.c.*

injections were performed directly into the psoriatic inflammatory skin (lesion site) or the distal area from the diseased site (non-lesion site), respectively. Twenty-four hours after the 2nd *s.c.* injection, the mRNA levels of TNF-α (B) and IL-6 (C) were evaluated. The relative transcript levels of TNF-α and IL-6 in each group to those in the IMQ (+) group are presented. Data are mean ± S.D. (n=3). * $P<0.05$.

Fig. 7. Amelioration of epidermis hyperplasia by etanercept delivered via IP in psoriasis model rats.

Etanercept (1 mg dose/rat) was transdermally (IP) or subcutaneously administered 5 and 7 days after the start of IMQ treatment. Eight days after the start of IMQ treatment, the 10-μm frozen skin sections were prepared and stained with HE. Microscopic images of skin sections from normal (A; n=3), IMQ-treated psoriasis model rats (B; n=4), the model rats treated with etanercept administered by IP (C; n=4) or *s.c.* injection (D; n=4). Scale bars = 100 μm. From the images of HE-stained skin sections, epidermis thickness of each group of rats was measured (E). Data are mean ± S.D. (n=4). ** $P<0.01$, *** $P<0.001$.

Table 1. Primer sequences for real-time RT-PCR.

Gene	Forward	Reverse
GAPDH	CCCCCAATGTATCCGTTGTG	TAGCCCAGGATGCCCTTTAGT
TNF-α	CGTAGCAAACCACCAAGCA	CGTAGCAAACCACCAAGCA
IL-6	TCCTACCCCAACTTCCAATGCTC	TTGGATGGTCTTGGTCCTTAGCC